Food Research International 157 (2022) 111354

Contents lists available at ScienceDirect

Food Research International

journal homepage: www.elsevier.com/locate/foodres

Integrated metabolomics of "big six" *Escherichia coli* on pea sprouts to organic acid treatments

Yue Wang [a,b], Xianfu Gao [c], Hongshun Yang [a,b,*]

[a] Department of Food Science and Technology, National University of Singapore, Singapore 117542, Singapore
[b] National University of Singapore (Suzhou) Research Institute, 377 Lin Quan Street, Suzhou Industrial Park, Suzhou, Jiangsu 215123, PR China
[c] Shanghai Profleader Biotech Co., Ltd, Jiading District, Shanghai 201805, PR China

ARTICLE INFO

Keywords:
Organic acid
Escherichia coli
Fresh produce
Foodomics
NMR
UPLC-MS
Sanitization
Food safety

ABSTRACT

Naturally occurring organic acids (OAs) have demonstrated satisfactory effects in inhibiting common pathogens on fresh produce; however, their effectiveness on "big six" *Escherichia coli* serotypes, comprised of *E. coli* O26:H11, O45:H2, O103:H11, O111, O121:H19 and O145, remained unaddressed. Regarding this, using nuclear magnetic resonance (NMR) spectroscopy and ultra-high performance liquid chromatography-mass spectrometry (UPLC-MS), the sanitising efficacy and the underlying antimicrobial mechanisms of 10-min treatments with 0.2 mol/L ascorbic acid (AA), citric acid (CA) and malic acid (MA) against the "big six" strains on pea sprouts were thoroughly investigated in this study.

Despite the varying antimicrobial efficacy (AA: 0.12–0.99, CA: 0.36–1.72, MA: 0.75–3.28 log CFU/g reductions), the three OAs induced consistent metabolic changes in the *E. coli* strains, particularly in the metabolism of membrane lipids, nucleotide derivatives and amino acids. Comparing all strains, the most OA-resistant strain, O26 (0.36–1.12 log CFU/g reductions), had the largest total amino acids accumulated to resist osmotic stress; its ulteriorly suppressed cell activity further strengthened its endurance. In contrast, the lowest OA-resistance of O121 (0.99–3.28 log CFU/g reductions) might be explained by the depletion of putrescine, an oxidative stress regulator. Overall, the study sheds light on the effectiveness of a dual-platform metabolomics investigation in elucidating the metabolic responses of "big six" *E. coli* to OAs. The manifested antimicrobial effects of OAs, especially MA, together with the underlying metabolic perturbations detected in the "big six" strains, provided scientific basis for applying OA treatments to future fresh produce sanitisation.

1. Introduction

With vigorous promotion of the health benefits of fresh produce by the World Health Organization (WHO) (World Health Organization, 2003, 2014), global awareness of increasing fresh produce consumption has been raised in recent years (Rekhy & McConchie, 2014). Concomitantly, foodborne outbreaks related to fresh produce consumption are also on the rise (Dewey-Mattia et al., 2019; Food and Drug Administration, 2022). Shiga toxin-producing *Escherichia coli* (STEC) are amongst the pathogens commonly contaminating fresh produce (Dewey-Mattia et al., 2018). According to the Centers for Disease Control and Prevention (CDC), in the past decade, they are responsible for 13 fresh produce-related foodborne outbreaks within the U.S. (https://www.cdc.gov/ecoli/outbreaks.html). Among the causative STEC serotypes, O157 is the most familiar to the public; for many years, it dominated the cause of life-threatening STEC infections and relevant food product recalls (Chung, Cho, & Rhee, 2018; Deng et al., 2011; Wang et al., 2009). Apart from O157, six emerging STEC serotypes combinedly known as "big six", including O26, O45, O103, O111, O121 and O145, are also noteworthy causes of the outbreaks. For instance, O26 was responsible for the 29 infections during a multistate outbreak linked to sprouts consumption in 2012 (Centers for Disease Control and Prevention, 2012). Moreover, O121 and O103 were the culprits of two additional sprouts-related outbreaks in 2014 and 2020, respectively, which together led to 70 infections and 10 hospitalisations (Centers for Disease Control and Prevention, 2014, 2020). Regarding the high occurrence and severity of the "big six" outbreaks related to fresh produce consumption, effective sanitisation approaches targeting "big six" are urgently needed by the fresh produce industry to protect consumer safety.

* Corresponding author at: Department of Food Science and Technology, National University of Singapore, Singapore 117542, Singapore.
E-mail address: fstynghs@nus.edu.sg (H. Yang).

https://doi.org/10.1016/j.foodres.2022.111354
Received 16 February 2022; Received in revised form 27 April 2022; Accepted 6 May 2022
Available online 10 May 2022

Organic acids (OAs) are potential sanitisers to achieve this goal. To date, many of the generally recognised as safe (GRAS)-affirmed OAs have demonstrated sanitising capability against common microbes in foods (Olaimat et al., 2017). For instance, Guo et al. (2022) reported 1.7–2.5 log reductions of *Salmonella enterica* strains on cucumber slices by 1% citric acid (CA). Besides, both acetic acid and lactic acid were proven to effectively inhibit the growth of *E. coli* O157:H7 in beef products (Fang & Tsai, 2003; Shen et al., 2011). Additionally, a range of OAs, including CA, malic acid (MA), propionic acid, lactic acid and acetic acid, exhibited significant antibacterial effects against *E. coli* O157, *Salmonella*, and *Listeria monocytogenes* on organic apples, lettuce and spinach at low concentrations in studies by Neal et al. (2012) and Park et al. (2011). These reported antimicrobial effects on common microbes suggested that OAs might be useful for "big six" inhibition as well.

In this study, the antimicrobial effects of three plant-derived OAs were specifically investigated. These were ascorbic acid (AA), which is ubiquitous in fruits and vegetables, CA, which exists notably in citric fruits, and MA, which is the main acid in apples, apricots, berries, grapes and pears (https://fdc.nal.usda.gov/). As the three OAs are naturally occurring in fresh produce, they seem to be more compatible with fresh produce application compared to OAs from other sources, such as acetic acid and propionic acid. In this way, once proven effective, they would be more easily popularised in the fresh produce industry.

The mechanisms of the potential bactericidal effects of the three OAs were also interested. Metabolomics, with the ability to acquire "snapshots" of metabolite profiles of bacterial cells at different cellular states, is increasingly utilised for mechanism study (Chen et al., 2020b). Nuclear magnetic resonance (NMR) spectroscopy and ultra-high performance liquid chromatography-mass spectrometry (UPLC-MS) are two of the metabolomic techniques practically used; while the former shows superiority in terms of reproducibility, non-destructiveness and non-invasiveness (Emwas, 2015), with recent application in identifying the metabolic disturbance in *E. coli* in sprouts under electrolysed water treatment (Wang, Wu, & Yang, 2022), the latter offers an ingenious unification of the high resolution of chromatography and the high sensitivity of MS for the analysis of complex biological systems (Ashraf et al., 2020), which thus has been applied to diagnose the metabolic biomarkers in microbes under a wide range of stresses, such as heat, oxidation as well as nutrient limitation (Ji et al., 2018; Lin et al., 2016; Tian et al., 2018). In light of the respective advantages associated with each technique, a parallel measurement by NMR and UPLC-MS may provide comprehensive insights into the metabolic responses of the "big six" *E. coli* strains in fresh produce toward the OA treatments.

Overall, in this work, the sanitising effects of three chosen OAs, AA, CA and MA, against "big six", were examined *in vivo*, using pea sprouts as the food matrix. Besides, through a dual-platform metabolomics investigation using the NMR and UPLC-MS techniques that complement each other, the metabolic changes in the strains underlying the OA antimicrobial processes were thoroughly elaborated at the molecular level. The results of the study would provide scientific basis for applying the plant-derived OA treatments in future fresh produce sanitisation.

2. Materials and methods

2.1. E. coli strains and culture condition.

Six *E. coli* strains, including *E. coli* O26:H11 (ATCC BAA-2196), O45:H2 (ATCC BAA-2193), O103:H11 (ATCC BAA-2215), O111 (ATCC BAA-2440), O121:H19 (ATCC BAA-2219) and O145 (ATCC BAA-2192), were utilised as representatives of "big six" to enable comparison of the responses of different *E. coli* serotypes to OAs. The strains (stored in 30% glycerol under − 80 °C) were obtained from the Department of Food Science and Technology, National University of Singapore. They were activated by inoculation into 10 mL of tryptone soya broth (TSB, Sigma-Aldrich, St. Louis, MO, USA) and incubated overnight at 37 °C. The activated strains were then adapted to 100 μg/mL of nalidixic acid (Sigma-Aldrich, St. Louis, MO, USA) via consecutive transfers with stepwise increments in nalidixic acid concentration. All media used in this study were also supplemented with 100 μg/mL of nalidixic acid accordingly to avoid interference of the naturally existing microbiota on pea sprouts (Kharel et al., 2018). Working cultures of individual strains were prepared by inoculating the adapted cultures into 10 mL of fresh TSB (1:100, v/v) with subsequent incubation at 37 °C overnight. Cell pellets were centrifuged at 4,500 × *g* for 10 min (20 °C), washed twice with 0.1% peptone water (Sigma-Aldrich, St. Louis, MO, USA) and finally harvested in 200 μL of 0.1% peptone water for pea sprouts inoculation.

2.2. Sample inoculation

Pea sprouts were purchased from a local supermarket in Singapore within 24 h before use and kept at 4 °C. Upon gentle rinsing for 60 s by cold tap water to remove undesired residues, those with no visible damage were air-dried and weighed into 10-g portions. Each weighed sample was spot inoculated with *E. coli* by aseptically depositing the 200 μL of concentrated cell suspension prepared in *2.1* with a micropipette at 10 to 15 locations on the surface. The method could ensure complete pellet delivery (Beuchat et al., 2017; Blessington, Theofel, & Harris, 2013), and led to homogeneous initial *E. coli* levels of approximately 8 log CFU/g across all samples. The six strains were inoculated individually, and each strain was inoculated on four samples for four different treatments. After inoculation, samples were air-dried in a laminar flow biosafety cabinet for at least 3 h to facilitate *E. coli* attachment.

2.3. Sanitising treatments

OAs were purchased from Sigma-Aldrich (St. Louis, MO, USA). Based on the FDA regulations (Title 21 CFR designation) and relevant studies (Allende et al., 2009; Chen et al., 2019; Min et al., 2007; Park et al., 2011), the AA, CA and MA treatment solutions were all prepared to a concentration of 0.2 mol/L by diluting in sterile deionised water (DW) to a final volume of 200 mL. The pH of the 0.2 mol/L AA, CA and MA solutions used in the study were 2.50 ± 0.02, 2.00 ± 0.01 and 2.10 ± 0.01, respectively, as determined by a pH meter (Orion 410, Thermo Scientific, Waltham, MA, USA) at room temperature.

The inoculated samples were randomly assigned to four treatment solutions: (I) 0.2 mol/L AA; (II) 0.2 mol/L CA; (III) 0.2 mol/L MA; (IV) DW (control). They were immersed in the solutions simultaneously at room temperature for 10 min to ensure that the full sanitising potential of the treatments was achieved. After that, samples were washed with 0.2 mol/L phosphate-buffered saline (PBS, pH 7.5) to neutralise the residual acids (Burnett & Beuchat, 2002; Chen et al., 2020b; Haskard, Binnion, & Ahokas, 2000). Successful neutralisation was confirmed by checking the pH of the final wash solution. Samples were then dried in the laminar flow biosafety cabinet for 30 min. Next, each sample was transferred to a sterile stomacher bag containing 90 mL of 0.1% sterile peptone water and homogenised for 180 s (Masticator Stomacher, IUL Instruments, Germany). Serial dilution was performed and 100 μL of diluent was plated on the nalidixic acid-supplemented tryptic soy agar (TSA, Sigma-Aldrich, St. Louis, MO, USA). The bacterial populations were counted after overnight incubation at 37 °C and the results were expressed as log CFU/g of the fresh weight. For each strain, the difference in viable populations between each OA treatment and the control was used to designate the sanitising efficacy of the OA.

2.4. Metabolite extraction and preparation for metabolomic analyses

For metabolomic analysis, each of the *E. coli* strains was conducted individually. To obtain sufficient *E. coli* cells for the extraction of metabolites, 200 g of inoculated pea sprouts were used for each treatment. After being immersed in specific treatment solutions for 10 min, the pea

Table 1
Reduction of *Escherichia coli* populations on pea sprouts under 10-min organic acid (0.2 mol/L) treatment.[a]

Serotype	Reduction of *Escherichia coli* population (log CFU/g)			
	AA	CA	MA	All treatments
O26	$^{A}0.12 \pm 0.05^{a}$	$^{A}0.36 \pm 0.08^{b}$	$^{A}0.74 \pm 0.18^{c}$	$^{A}0.41 \pm 0.29$
O45	$^{AB}0.26 \pm 0.04^{a}$	$^{D}1.72 \pm 0.07^{b}$	$^{B}1.90 \pm 0.15^{c}$	$^{D}1.29 \pm 0.79$
O103	$^{B}0.37 \pm 0.15^{a}$	$^{BC}0.87 \pm 0.04^{b}$	$^{B}2.05 \pm 0.07^{c}$	$^{BC}1.10 \pm 0.75$
O111	$^{B}0.36 \pm 0.04^{a}$	$^{B}0.82 \pm 0.16^{b}$	$^{B}1.97 \pm 0.03^{c}$	$^{B}1.05 \pm 0.73$
O121	$^{C}0.99 \pm 0.10^{a}$	$^{C}1.02 \pm 0.06^{a}$	$^{D}3.28 \pm 0.17^{b}$	$^{E}1.76 \pm 1.14$
O145	$^{A}0.11 \pm 0.08^{a}$	$^{BC}0.88 \pm 0.01^{b}$	$^{C}2.49 \pm 0.14^{c}$	$^{C}1.16 \pm 1.05$
Total	0.37 ± 0.31^{a}	0.95 ± 0.42^{b}	2.07 ± 0.79^{c}	

[a] AA: ascorbic acid; CA: citric acid; MA: malic acid. Data are presented as means ± standard deviation (n = 3). Values for the same treatment within each column preceded by different uppercase letters are significantly different ($P < 0.05$). Values for the same serotype within each row followed by different lowercase letters are significantly different ($P < 0.05$).

sprout samples were kneaded for 30 s to dissociate the *E. coli* cells. Afterwards, treatment solutions were collected and centrifuged at 500*g* for 3 min (4 °C) to precipitate pea sprouts debris. *E. coli* cells were harvested from the solutions by centrifugation at 12,000*g* for 10 min (4 °C), washed once with 0.2 mol/L PBS (pH 7.5) and twice with 0.1% peptone water (Zhao et al., 2020). Upon collection, the cell pellets were dried with clean nitrogen flow and immediately mixed with 1 mL of ice-cold methanol-d_4 (Cambridge Isotope Laboratories, Tewksbury, MA, USA) for NMR analysis or ice-cold LC-MS grade methanol (Waters, Milford, MA, USA) for UPLC-MS analysis to cease cellular enzymatic activities and quench metabolomic changes (Sellick et al., 2011). Complete cell lysis was achieved through three freezing-thawing cycles where the mixture was frozen in liquid nitrogen and thawed on ice (Chen et al., 2020b; Jäpelt et al., 2015; Winder et al., 2008). The mixture was then kept at – 20 °C for overnight metabolite extraction before subjecting to high-speed centrifugation at 12,000*g* (20 min, 4 °C). For NMR analysis, the obtained supernatant was collected, spiked with 1 mM trimethylsilyl propanoic acid (TSP; Sigma-Aldrich, Singapore; internal standard), and transferred into a 5 mm NMR tube (Sigma-Aldrich, St. Louis, MO, USA). For UPLC-MS analysis, the supernatant was spiked with 0.1 mM gallic acid (Sigma-Aldrich, Singapore) before being injected through a sterile nylon 0.22 μm filter (Waters, Milford, MA, USA) into the HPLC vial. Quality control (QC) samples were also prepared for UPLC-MS analysis, by pooling equivalent aliquot of all samples (Loh et al., 2021).

2.5. NMR analysis

The procedures for NMR analysis were adapted from our previous works (Lou, Zhai, & Yang, 2020; Wang, Wu, & Yang, 2022). The Bruker DRX-500 NMR spectrometer (Bruker, Rheinstetten, Germany) was used to scan the samples via a Triple Inverse Gradient probe. The ^{1}H spectra with a width of 10 ppm were obtained using the standard Bruker NOESY pulse sequence (noesypr1d). Prior to Fourier transformation, the free induction decays were multiplied by an exponential function equivalent to a 1-Hz line-broadening factor. Besides, the 2D ^{1}H–^{13}C heteronuclear single quantum coherence (HSQC) spectra of two representative samples were acquired to facilitate metabolite identification. Using the Bruker hsqcedetgpsisp2.3 pulse sequence, the ^{1}H spectra (10-ppm width) and ^{13}C spectra (180-ppm width) were obtained in F2 and F1 channels, respectively (Zhao et al., 2019).

2.6. UPLC-MS analysis

Samples were analysed by the ACQUITY UPLC^{TM} I-Class PLUS system (Waters, Milford, MA, USA) coupled to a VION ion mobility spectroscopy quadrupole time-of-flight mass spectrometer (IMS-QTOF-MS) (Waters, Manchester, U.K.), with an electrospray ionization (ESI) source operating in both positive (ESI^{+}) and negative (ESI^{-}) modes. An ACQUITY UPLC HSS T3 column (2.1 × 100 mm, 1.8 μm; Waters, Singapore) with temperature maintained at 30 °C was used to separate metabolites. The sample flow rate was set at 0.3 mL/min. The mobile phase consisted of 0.1% formic acid (FA) in water (Honeywell Burdick & Jackson, Muskegon, MI, USA) (A) and acetonitrile (Honeywell Burdick & Jackson, Muskegon, MI, USA) (B), and gradient conditions were as follows: 0–1.5 min 5% B, 1.5–3 min 5–50% B, 3–13 min 50–80% B, 13–13.5 min 80 – 95% B, 13.5 – 16 min 95% B, 16–16.1 min 95–5% B, and 16.1–20 min 5% B.

The capillary voltage was 2.0 kV for positive mode and 2.5 kV for negative mode. Nitrogen was used for desolvation, nebulisation and collision. The source temperature was set to 100 °C and desolvation gas to 500 °C with a flow rate of 800 L/h. The mass spectrometer was operated in accurate mass screening mode for QC data acquisition in both ionization modes and MS^{E} for all samples. The MS^{E} experiments acquired two acquisition functions simultaneously over an *m/z* range of 50–1200 Da at a scan time of 0.2 s. A low-energy function with a fixed collision energy of 4 eV and a high-energy function with a collision energy ramp from 20 to 40 eV were adopted. For automated mass measurement, a leucine enkephalin solution (50 ppb) in acetonitrile/H_2O (50:50, v/v) containing 0.1% FA was infused at 10 μL/min through a lockspray needle and acquired every 5 min with a scan time of 0.2 s. The protonated and deprotonated forms of leucine enkephalin were used for lock-mass corrections at *m/z* 556.2771 and 554.2620 in ESI^{+} mode and ESI^{-} mode, respectively, to ensure accurate mass measurements along runs (Loh et al., 2021).

2.7. Spectral analysis

For all NMR spectra, baseline correction and phase distortion adjustment were manually conducted on TopSpin 4.0.9 (Bruker). 1D ^{1}H and 2D ^{1}H–^{13}C spectra were used cooperatively for metabolite identification, where the Madison Metabolomics Consortium Database (MMCD), the Human Metabolome Database (HMDB) as well as relevant studies were referred for identity confirmation. The full resolution ^{1}H spectra (0.5–10.0 ppm) excluding the methanol region (3.26–3.36 ppm) were normalised to the sum intensities and binned into baskets with 0.02 ppm integral width using Mestrenova (Mestreab Research SL, Santiago de Compostela, Spain). The binned spectral data were first subject to principal component analysis (PCA) and hierarchical cluster analysis (HCA) for group separation. Moreover, pairwise comparison was performed by the supervised orthogonal projection to latent structures-discriminant analysis (OPLS-DA) to identify the significantly altered metabolites in each OA treatment compared to the control (SIMCA 14.1, Umetrics, Umeå, Sweden), using the selection criteria of variable importance in projection (VIP) > 1 and P value < 0.05 (Chen et al., 2020a).

The UPLC-MS spectra were processed using the Progenesis QI software (V.2.4, Nonlinear Dynamics, Waters, Newcastle, U.K.), on which baseline filtering, retention time alignment, 3D peak picking and response normalisation were automatically performed. For metabolite identification, the adducts $[M + H]^{+}$, $[M + NH_4]^{+}$, $[M + Na]^{+}$ and $[M + K]^{+}$ were selected for the positive mode, and $[M - H]^{-}$ and $[M - H_2O - H]^{-}$ were selected for the negative mode, and the *E. coli* Metabolome Database (ECMDB), the Kyoto Encyclopedia of Genes and Genomes (KEGG) database as well as the HMDB were collectively used for reference. PCA and OPLS-DA of the spectral data were further carried out on the EZinfo (V.3.0, Umetrics, Sweden). The significantly altered metabolites in each OA-treated sample compared to the control (VIP > 1, P value < 0.05 and CV ≤ 30) were carefully screened out. They were combined with those obtained from NMR analysis for interpretation of the main metabolic perturbations in the *E. coli* strains induced by the OA treatments.

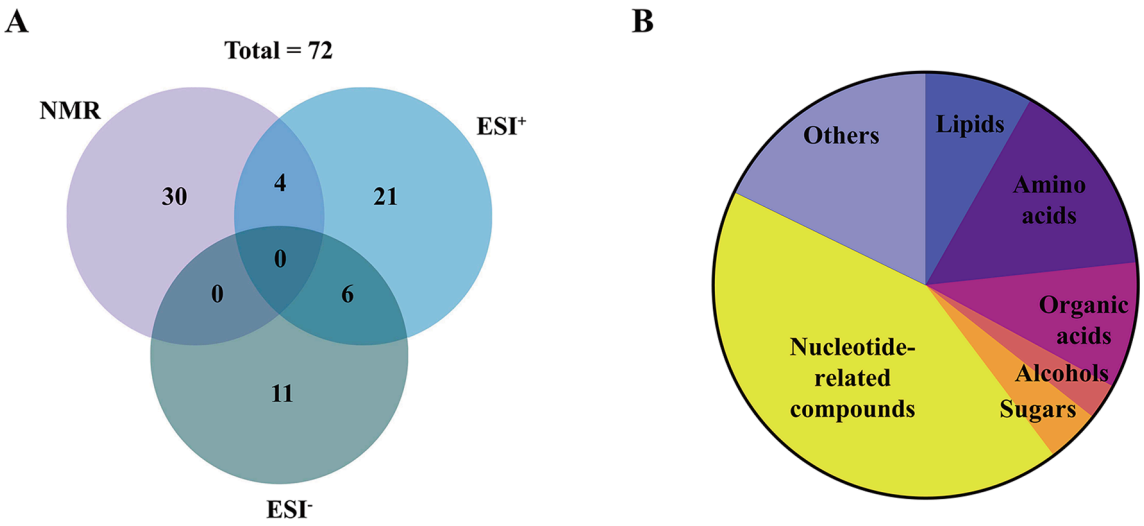

Fig. 1. Venn diagram showing the overlap of metabolites detected by NMR and UPLC-MS (A); metabolite composition of the *Escherichia coli* strains (B).

2.8. Statistical analysis

All tests were performed on at least three replications, where each replication was treated as an independent and autonomous experiment using separately inoculated cultures. Analysis of variance (ANOVA) and the least significant difference (LSD) were performed on SAS 9.4 (Statistical Analysis System, Cary, NC, USA) to compare the sanitising efficacy of the different treatments against the six *E. coli* strains. Differences with a P value < 0.05 were considered to be statistically significant.

3. Results and discussion

3.1. Reduction of E. coli on pea sprouts under different organic acid treatments

The antimicrobial efficacy of the OAs against the "big six" strains, including O26:H11 (ATCC BAA-2196), O45:H2 (ATCC BAA-2193), O103:H11 (ATCC BAA-2215), O111 (ATCC BAA-2440), O121:H19 (ATCC BAA-2219) and O145 (ATCC BAA-2192), on pea sprouts is shown in Table 1. Among the three OAs, MA was no doubt the most effective, which reduced all strains, except for O45, by double or even triple amounts (0.74–3.28 log CFU/g) that were reduced by CA. CA ranked number two in sanitising efficacy, leading to reductions of the "big six" strains by 0.36–1.72 log CFU/g. Both MA and CA have demonstrated satisfactory anti-*E. coli* effects previously. For instance, Park et al. (2011)'s finding that a 10-min treatment with either 0.075 mol/L MA or 0.05 mol/L CA mitigated *E. coli* O157:H7 by over 2.2 log CFU/g on sprouts and by over 1.5 log CFU/g on apples illuminated the effectiveness of the two OAs at very low levels. Compared to MA and CA, the inhibitory efficacy of AA seemed to be trivial. Except for the relatively high reduction achieved in O121 (0.99 log CFU/g), reductions of all the other strains by AA were kept below 0.37 log CFU/g. This inconspicuous sanitising power suggested that AA might be more of a nutritional supplement than a sanitiser if it was applied to foods.

For each strain, the resistance to the different OAs was interlinked. The most resistant strain to MA, O26, for instance, showed superiority in surviving AA and CA as well, diminished by <0.75 log CFU/g from all three treatments (Table 1). At the opposite extreme, O121 was generally the most vulnerable towards the OA attacks (0.99–3.28 log CFU/g reductions); only under CA treatment was its reduction significantly exceeded by O45 ($P = 0.001$). Additionally, O103 and O111 exhibited comparable sensitivity to each other under the same treatment, and thus, similarity in their stress defence mechanisms was suspected. Overall, despite the varying sanitising power among the three OAs, the strains' different resistance to the OA stresses in general could be identified. To unravel the ultimate reasons for the uneven OA-resistance among the strains, an investigation of their metabolic responses during OA application may be helpful.

3.2. Metabolic profiling of E. coli on pea sprouts by NMR and UPLC-MS

The NMR and UPLC-MS metabolomic techniques combinedly identified a total of 72 metabolites in the *E. coli* strains, which demonstrated a huge enhancement in metabolite coverage as compared to previous metabolomic analyses carried out by NMR or UPLC-MS alone (Chen et al., 2020b; Liu et al., 2020; Wang, Wu, & Yang, 2022; Wang, Zhou, & Yang, 2022). From Fig. 1A, except for four metabolites (i.e., phenylalanine, adenosine, NAD and ADP) jointed identified on both platforms, 21 and 11 unique metabolites were detected by UPLC-MS ESI^+ and ESI^-, respectively, while 30 specific metabolites were solely detected by NMR.

NMR is the golden technique for untargeted metabolomics, which is capable of generating metabolic profiles based on the complete set of metabolites of a biological sample (Emwas, 2015). In line with this, the set of metabolites annotated on the ^{1}H NMR spectra was an epitome of the complete *E. coli* metabolic profile, where amino acids, organic acids, alcohols, sugars and nucleotide derivatives have all been detected (Fig. S1-S4 and Table S1). In comparison, the UPLC-MS technique seemed to specialise in lipid and nucleotide detection (Fig. S5 and Table S2); however, it barely detected the metabolites with a polar nature, such as sugars, organic acids, alcohols, polyols and some amino acids, possibly due to the lack of retention and poor separation of important isomers in the reversed-phase LC system (Lioupi et al., 2021). Since the NMR technique is irrelevant to the polarity of metabolites, it offers a perfect complement to the metabolome probed by UPLC-MS. Overall, the composition of *E. coli* metabolites detected from the two platforms is presented in Fig. 1B. It can be seen that while nucleotide-related compounds accounted for almost half of the detected metabolites, amino acids, organic acids, lipids, sugars, alcohols and others collectively took up the other half.

3.3. Overall differences in metabolic profiles of E. coli on pea sprouts from different treatments

To obtain a global overview of the metabolic differences among *E. coli* strains from different treatments, PCA was conducted using the NMR, ESI^+ and ESI^- datasets.

The NMR data compared all groups (6 strains × 4 treatments) in a single PCA model. With the first three principal components (PCs)

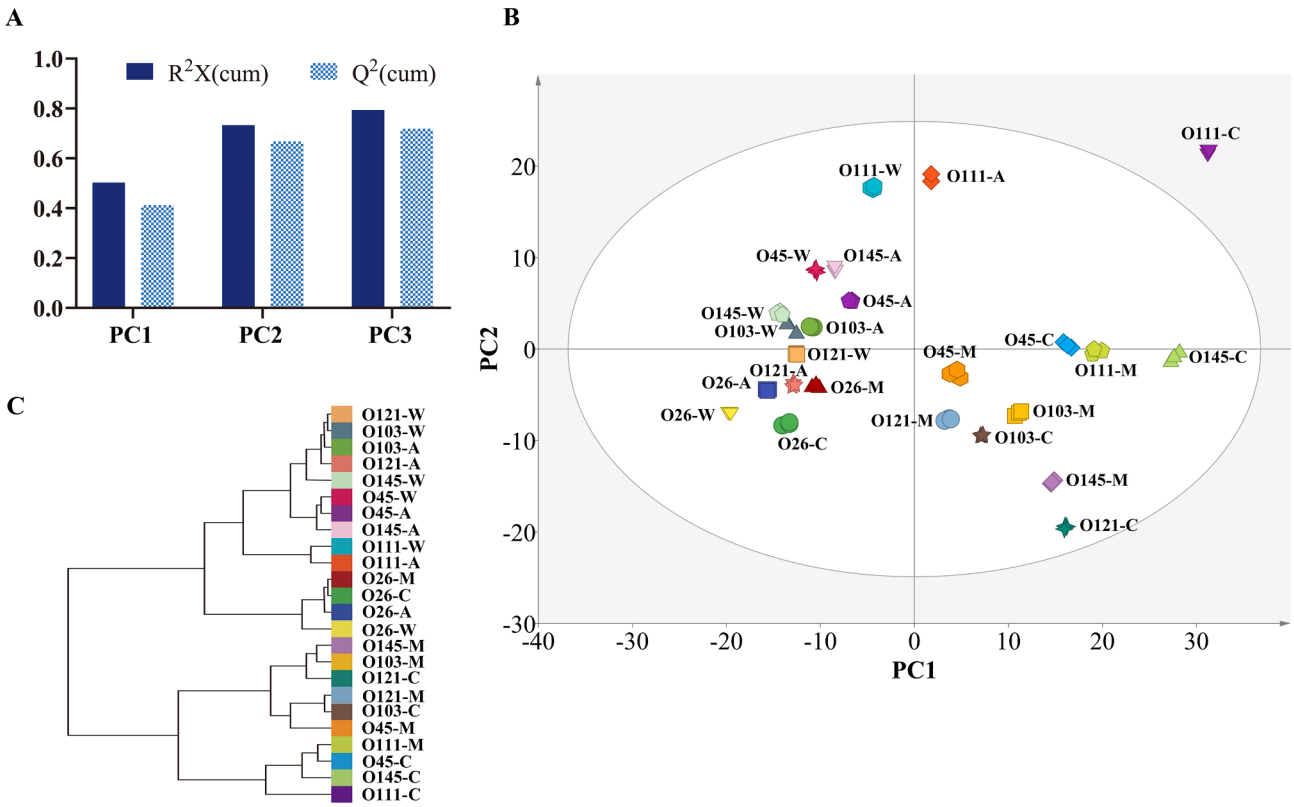

Fig. 2. Principal component analysis (PCA) of ^{1}H NMR spectra of *Escherichia coli* strains on pea sprouts. Principal components explaining for the variances (A); score plot (B); hierarchical clustering (C). Note: W: deionised water; A: ascorbic acid; C: citric acid; M: malic acid.

explaining 79.4% of the total variance (PC1: 50.3%, PC2: 23.0%, PC3: 6.1%) and the quality parameter Q^2 being much higher than 0.5 (Fig. 2A), the model demonstrated satisfactory predictivity and interpretability (He et al., 2021). The 24 groups showed clear separation on the score plot (Fig. 2B). Meanwhile, the triplicates from each group were tightly aggregated, indicating outstanding reproducibility of the samples prepared. The control samples of all strains were positioned close to each other spatially on the plot, suggesting the similarity of the metabolic status of the six strains originally. In contrast, the stressed samples were scattered in all directions, which manifested that drastic metabolic variations were induced by the OAs. Amongst the six strains, O26 demonstrated the meekest metabolic changes, for its metabolic profiles were confined to the same quadrant regardless of the treatment applied; this might be the inner embodiment of the strain's low sensitivity to the OA stresses.

Using the NMR dataset, HCA based on Euclidean distance and Ward algorithm was further performed for a more sophisticated classification of the groups. Two major categories were illustrated on the dendrogram (Fig. 2C). Congruent with the observations on the PCA score plot, all the control samples were grouped into the same category. In addition, all the AA-treated ones were also assigned to this category, revealing relatively mild stimulation of AA on the strains at the metabolic level. The other major category, in contrast, was exclusively comprised of the CA- and MA-treated samples; no clear demarcation was observed between the two treatments, whereby some internal coherence in their antimicrobial mechanisms was suspected.

Twelve PCA models were built separately using the UPLC-MS ESI^+ and ESI^- datasets. All models showed good fitness to the data based on the R^2X (close to 1) and Q^2 (>0.5) accumulated by the first 5 PCs (Table S3). Moreover, as the QC samples were correctly located in the centre of most score plots (Fig. 3), good data quality was ensured (Loh et al., 2021). For all strains, the metabolomes of the unstressed cells were distant from those stressed on the score plots, which ascertained that the change of the *E. coli*'s metabolomes induced by OAs was effectively captured on the UPLC-MS platform. Besides, the metabolomes of *E. coli* from the CA and MA treatments were closely positioned in both modes of detection, implying that similar trends of metabolic changes might have been stimulated by the two OAs. This was consistent with that observed from the NMR analysis mentioned above, which suggested that the results obtained from the two metabolomic techniques could be mutually authenticated.

3.4. Altered metabolites in *E. coli* on pea sprouts by different organic acid treatments

To elucidate the detailed metabolic changes induced by OAs in the *E. coli* strains, the significantly altered metabolites after each OA treatment were identified by OPLS-DA. The NMR spectral data were well fitted to the OPLS-DA models (R^2Y: 0.95 – 0.99, Q^2: 0.82 – 0.99). S-plots were generated based on the covariance, p, and correlation, p(corr), between the metabolites and the modelled class designation, where points below and above the x-axis indicated features with lower and higher signals in the control sample (Fig. 4, Fig. S6-S7). Metabolites with VIP > 1 that made credible contributions to the separation of the paired samples were highlighted at the far left or right sides (coloured in red) on the plots (Wiklund et al., 2008). They were further screened based on the *P* values to enable the diagnosis of the metabolites that significantly differentiated each stressed-and-unstressed sample pair (Table 2). All metabolites detected from UPLC-MS were also screened in this way, where those significantly altered after the OA treatments are summarised in Table 3. From the Tables, it can be seen that both platforms were able to capture the strain-specific metabolic changes under the OA stresses. To aid comparison among the strains, a full list of the significantly discriminative metabolites identified is provided in Fig. 5, with arrows pointing upwards and downwards highlighting increasing and decreasing contents after each OA stress. Based on these metabolites, an

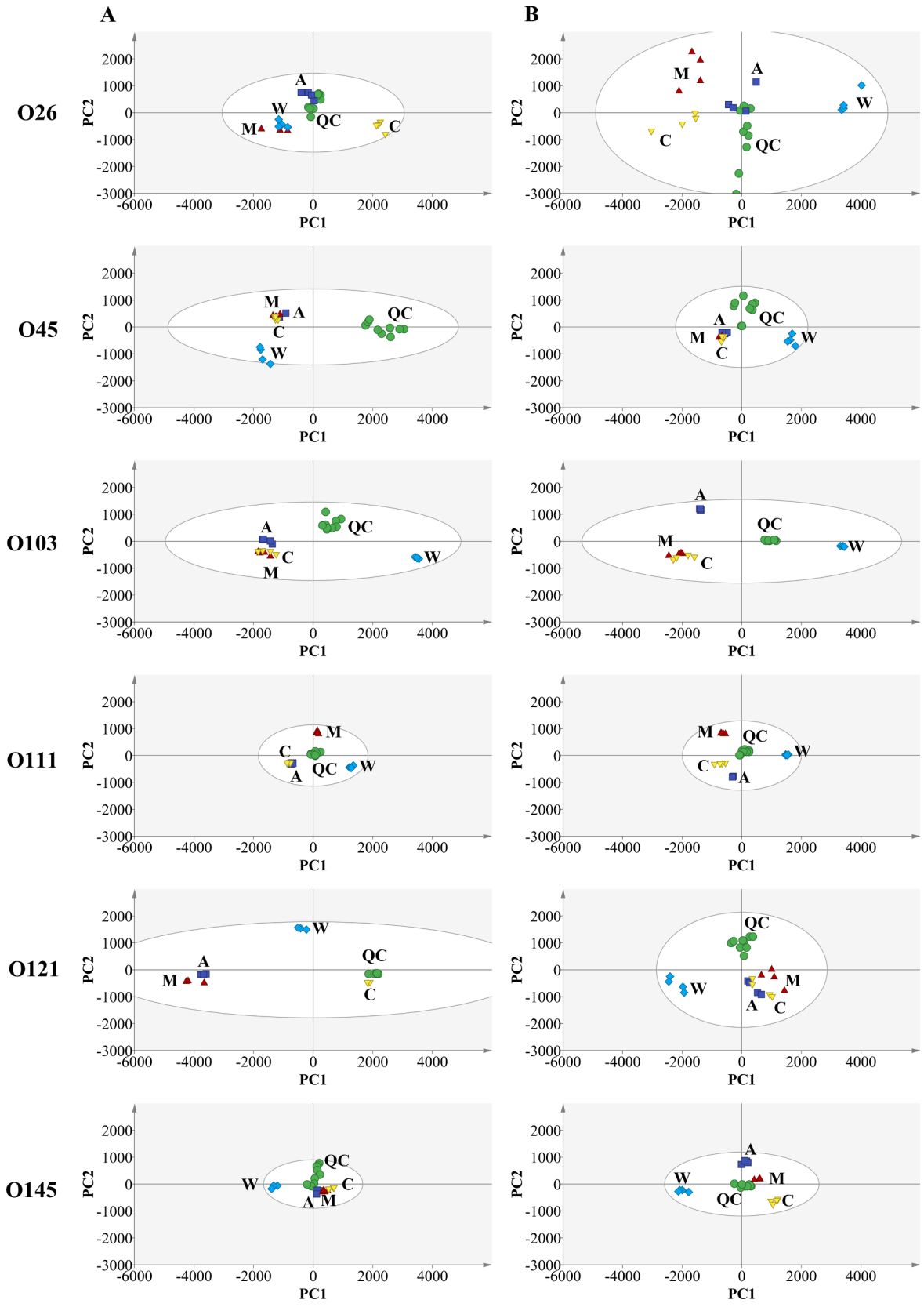

Fig. 3. Principal component analysis (PCA) of UPLC-MS spectra of *Escherichia coli* strains on pea sprouts. Score plots from the positive mode of detection (ESI^+) (A); score plots from the negative mode of detection (ESI^-) (B). Note: W: deionised water; A: ascorbic acid; C: citric acid; M: malic acid; QC: quality control.

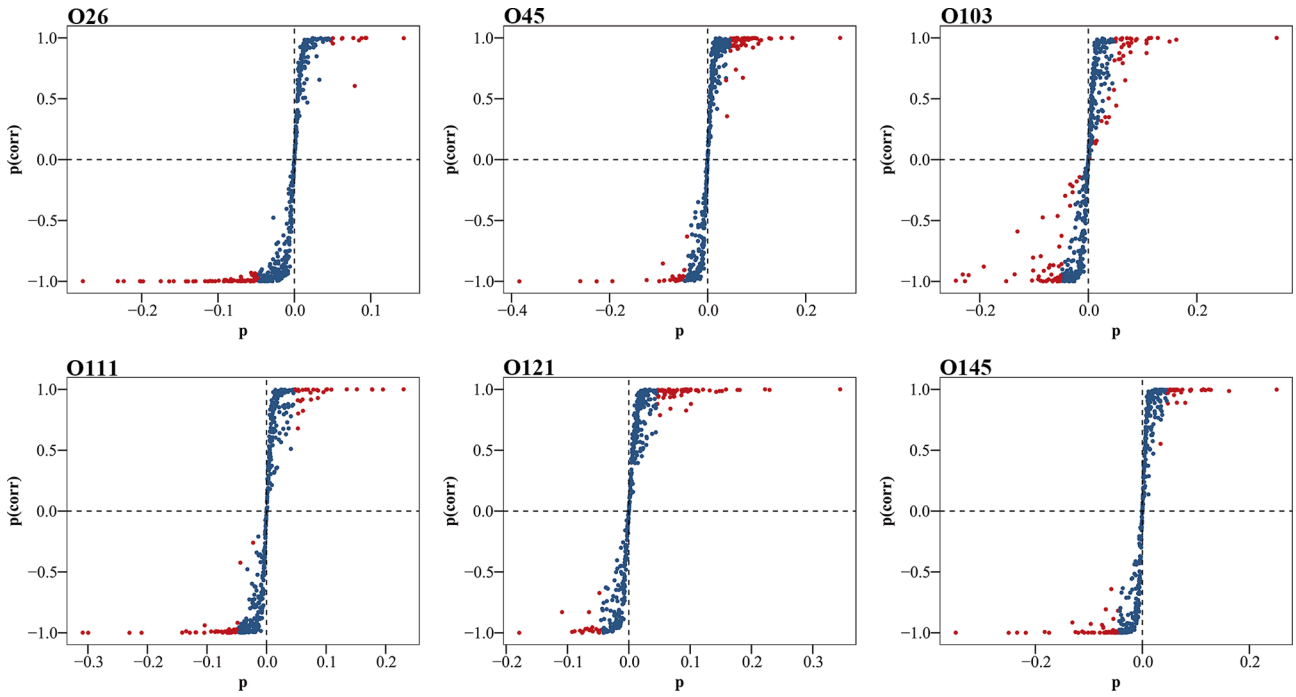

Fig. 4. Orthogonal partial least squares discriminant analysis (OPLS-DA) S-plots of NMR analysis of *Escherichia coli* strains from deionised water-treated and 0.2 mol/L ascorbic acid-treated pea sprouts.

assumptive schematic map showing the major perturbations in the *E. coli*'s metabolic networks is proposed in Fig. 6 to facilitate rationalisation of the strains' different resistance against OAs in the following section.

3.5. Metabolic network perturbations in *E. coli* on pea sprouts under organic acid treatments

3.5.1. Lipid metabolism

For all bacteria, cell membrane is the first barrier encountering extracellular stresses. Concomitantly, remarkable changes in an array of membrane lipids were observed in the OA-stressed strains, showing a general upward trend (Fig. 5; Fig. 6). Among the significantly discriminative lipids ($P < 0.05$), lysophosphatidylethanolamine (LPE) is the hydrolysed product of the most dominant cell membrane constituent, phosphatidylethanolamines (PE) (Tepperman & Soper, 1999). Conversion of LPE from PE typically happens during activities that compromise the integrity of cell membranes, such as heat shock (de Geus et al., 1983; Tian et al., 2018), T4 phage infection (Cronan Jr & Wulff, 1969), and exposure to antimicrobial lipopeptide (Wright et al., 1990), marking the beginning of *E. coli* cell lysis (Weiss, Beckerdite-Quagliata, & Elsbach, 1979). Similarly, lysophosphatidylglycerol (LPG) and Lysophosphatidylcholines (LPC) are also derived by hydrolysis of major membrane phospholipids, from phosphatidylglycerol (PG) and phosphatidylcholines (PC), respectively (Zheng et al., 2017). In our work, from the elevated levels of all three lysophospholipids, cell membrane impairment was highly suspected in the OA-stressed *E. coli* strains. Besides, a significant decline in phosphorylcholine was observed in the AA-stressed O121 and O145 cells. As phosphorylcholine is a key membrane phospholipid precursor (Geiger, López-Lara, & Sohlenkamp, 2013), its reduction provided additional evidence of a weakened membrane structure.

Elevation in osmotic stress might be responsible for the weakened membrane under the OA treatments. Based on a prevailing opinion, as weak acids, OAs can cross the bacterial cell membrane freely in the undissociated form and dissociate once inside the cell (Brul & Coote, 1999; Olaimat et al., 2022; Salmond, Kroll, & Booth, 1984). The released anions are trapped in the cytoplasm and accumulated, which increases the ionic strength and osmotic stress (Russell, 1992). The osmotic stress subsequently causes irreversible damage to the *E. coli*'s morphology (Alemohammad & Knowles, 1974; Wood, 1999), with the formation of small vesicles on the cell membrane being the most evident change (Mille, Beney, & Gervais, 2002). Previous studies have also documented the impairment of *E. coli* cell membrane towards OA treatments. For instance, in Chen et al. (2022)'s study where *E. coli* O157 treated with 2% lactic acid was viewed under the atomic force microscope, a severely impaired outer membrane that exposed the inner membrane of the cells has been observed. Additionally, Zhang et al. (2019)'s study also highlighted membrane impairment as a cause of the death of *E. coli* O157 under octanoic acid treatment. Combining these with our results, cell membrane disintegration is a key disinfectant mechanism of OAs on the *E. coli* cells.

3.5.2. Nucleotide metabolism

Inside the cells, nucleotides presented a consistent alteration pattern among the six strains (Fig. 5; Fig. 6). For instance, a uniform reduction in NAD (exists as NAD^+ or NADH) was observed. NAD is a ubiquitous coenzyme participating in hundreds of enzymatic oxidation–reduction reactions (Dong et al., 2014; Foster & Moat, 1980; Ozment et al., 1999), and thus, the drop in its content revealed a compromise in virtually all metabolic pathways in a living cell. Previous studies have documented the switch of *E. coli* cells from exponential growth to stationary-phase growth under adverse environmental conditions (Kanjee & Houry, 2013; Liu et al., 2017). The lowering of NAD observed in this study, therefore, indicated that this energy-saving strategy was also adopted for OA stress endurance. During this phase, the intracellular metabolic activities were constrained to the most essential functions only, whereas those irrelevant to maintaining basal metabolism were depressed (Gray et al., 2019; Kempes et al., 2017). For instance, with lower energy requirements, the metabolism of glucose, the core energy source in *E. coli*, was decreased, as evidenced by the significant declination of α-D-glucose, ethanol, lactic acid, acetic acid and 1,2-propanediol in most strains (Jain et al., 2015). Likewise, the synthesis of coenzyme A from pantothenic acid via the formation of dephospho-CoA was also retarded,

Table 2
Significantly differential metabolites ($P < 0.05$) in *Escherichia coli* strains on pea sprouts from each organic acid treatment in comparison to the control detected by NMR spectroscopy [a].

Serotype	Metabolite	AA		CA		MA	
		VIP	Trend	VIP	Trend	VIP	Trend
O26	Leu	3.05	↑**	2.56	↑**	2.87	↑**
	Ile	1.74	↑**	1.12	↑**	2.24	↑**
	Ethanol			1.72	↓*	1.20	↓*
	Lactic acid	5.95	↑**	4.63	↑**	6.47	↑**
	Acetic acid			2.26	↓**	1.81	↓**
	Glu	1.77	↑**			1.04	↑*
	Met	1.77	↑**			1.01	↑**
	Putrescine					2.60	↑**
	His			2.61	↓**	2.07	↓*
	Uridine	1.80	↑**	1.77	↑**	1.59	↑*
	Uracil	1.61	↑**	1.52	↑**	1.69	↑*
	Xanthine	2.37	↑**	2.47	↑**	2.13	↑**
	Hypoxanthine	1.94	↑**	2.11	↑**	1.98	↑**
O45	Leu	1.02	↑**	1.77	↑**		
	Ile	1.72	↓**	1.63	↓**		
	1,2-propanediol	1.26	↓**				
	Ethanol	2.14	↓*	3.07	↑**		
	Lactic acid	2.74	↓*	1.66	↓*	3.67	↓**
	Acetic acid	2.67	↓**	1.55	↓**	2.12	↓**
	Met			1.35	↓*	1.31	↓**
	Putrescine	4.13	↑**	2.80	↑**	2.30	↑*
	His	2.07	↓**	2.04	↓**	2.21	↓**
	Uridine	1.29	↑**	1.48	↑**	1.79	↑*
	Adenosine	1.21	↓*				
	α-D-glucose	1.26	↓**				
	Phe			1.06	↑**		
	Xanthine	1.89	↑**	1.69	↑**	2.10	↑**
	Hypoxanthine	1.88	↑**	1.67	↑**	2.05	↑**
O103	Leu					2.15	↑*
	Ile			1.86	↓*		
	Ethanol	3.26	↓*	1.84	↓*	1.75	↓*
	Lactic acid	4.73	↑**	2.58	↓*	3.08	↑*
	Arg	1.70	↑*				
	Acetic acid	3.03	↓**	2.03	↓**	1.88	↓**
	Glu	1.85	↑*			1.16	↑**
	Met	1.76	↑*	1.11	↓**	1.00	↓*
	His	1.60	↓*	2.05	↓**	1.85	↓**
	Uridine			1.21	↑**	1.24	↑**
	Adenosine			1.05	↓**		
	α-D-glucose	1.24	↓**				
	Phe	1.11	↑**				
	Uracil					1.09	↑**
	Xanthine	1.67	↑**	1.46	↑**	1.55	↑**
	Hypoxanthine	1.52	↑**	1.27	↑**	1.45	↑**
O111	Leu	1.99	↑**	2.62	↑**		
	Ile					2.50	↓**
	Ethanol	4.47	↑**	5.04	↑**	3.89	↑**
	Lactic acid	4.90	↑**	5.04	↑**	5.17	↓**
	Arg	1.32	↑*				
	Acetic acid	2.32	↓**	1.66	↓**	1.79	↓**
	Glu	1.08	↑**	1.35	↑**		
	Met			1.08	↓*	1.16	↓*
	Putrescine			2.36	↑**	2.11	↓**
	His	1.81	↓*			2.16	↓**
	Uridine	1.43	↑**	1.01	↑**	1.02	↑**
	Adenosine	1.48	↓**			1.03	↓**
	α-D-Glucose	1.06	↓*				
	Xanthine	1.85	↑**	1.25	↑**	1.23	↑**
	Hypoxanthine	1.81	↑**	1.25	↑**	1.22	↑**
O121	Leu	1.87	↓*	1.06	↑*	1.75	↑**
	Ile	2.34	↓**	2.04	↓**	2.04	↓**
	1,2-propanediol	1.47	↓*				
	Ethanol	2.39	↓*	2.82	↑**	1.93	↓*
	Lactic acid	4.90	↓**	3.57	↓**	2.25	↓**
	Arg	1.92	↑*				
	Acetic acid	3.39	↓**	1.30	↓**	1.74	↓**
	Met	1.60	↑**			1.28	↓**
	Putrescine	4.74	↓**	2.04	↓*		
	Phosphorylcholine	1.13	↓**				
	His	1.25	↓*	1.70	↓**	2.08	↓**
	Uridine	1.27	↑*			1.20	↑**
	Adenosine	1.53	↓**				

(*continued on next page*)

Table 2 (*continued*)

Serotype	Metabolite	AA		CA		MA	
		VIP	Trend	VIP	Trend	VIP	Trend
	α-D-glucose	1.39	↓**				
	Uracil					1.04	↑**
	Xanthine	1.88	↑**	1.17	↑**	1.50	↑**
	Hypoxanthine	1.97	↑**	1.09	↑**	1.47	↑**
O145	Leu	2.41	↑**	2.43	↑**	1.66	↑**
	Ile	2.68	↑**	1.05	↑*	1.98	↓**
	1,2-propanediol	1.34	↓**			1.14	↓**
	Ethanol			1.59	↑*		
	Lactic acid	4.47	↑**	4.65	↑**	3.61	↓**
	Arg					1.37	↓*
	Acetic acid	2.66	↓**	1.23	↓**	1.59	↓**
	Glu	1.96	↓**	1.04	↓*	1.62	↓**
	Met					1.23	↓**
	Putrescine	3.74	↓**	1.66	↑**	1.05	↑**
	Phosphorylcholine	1.21	↓**				
	His	1.53	↑**			1.86	↓**
	Uridine			1.07	↑**	1.06	↑**
	Uracil			1.04	↑**	1.28	↑**
	Xanthine	1.25	↑**	1.35	↑**	1.42	↑**
	Hypoxanthine	1.39	↑**	1.26	↑**	1.28	↑**

[a] AA: ascorbic acid; CA: citric acid; MA: malic acid; VIP: variable importance in projection. *$P < 0.05$, **$P < 0.01$.

Table 3
Significantly differential metabolites ($P < 0.05$) in *Escherichia coli* strains on pea sprouts from each organic acid treatment in comparison to the control detected by UPLC-MS [a].

Serotype	Metabolite	Polarity	AA		CA		MA	
			FC	Trend	FC	Trend	FC	Trend
O26	$NADP^+$	ESI^+	24.88	↓	∞	↓	∞	↓
	$NADP^+$	ESI^-	3.90	↓	39.94	↓	29.67	↓
	CMP	ESI^+	1.72	↓	4.82	↓	3.18	↓
	CMP	ESI^-	1.65	↓	2.84	↓	1.82	↓
	CMP-Neu5Ac	ESI^-	18.34	↓	655.91	↓	541.06	↓
	GDP-colitose	ESI^-			23.61	↓	13.79	↓
	ADP	ESI^+	6.05	↓	33.63	↓	16.19	↓
	cADP-ribose	ESI^+	6.08	↓	29.28	↓	13.34	↓
	cADP-ribose	ESI^-	5.79	↓	18.73	↓	9.78	↓
	NAD	ESI^+	11.50	↓	68.59	↓	29.96	↓
	AMP	ESI^+	1.55	↓	8.06	↓	6.78	↓
	Adenine	ESI^+	3.38	↓	27.15	↓	22.08	↓
	GMP	ESI^+			6.26	↓	5.60	↓
	dAMP	ESI^+			6.36	↓	6.60	↓
	Glutathione disulphide	ESI^+	7.53	↓	44.01	↓	22.05	↓
	c-di-GMP	ESI^-	2.12	↓	4.76	↓	3.78	↓
	Coenzyme A	ESI^-	24.39	↓	87.28	↓	95.15	↓
	Pantothenic acid	ESI^+	13.38	↓	84.62	↓	64.87	↓
	FMN	ESI^+	2.88	↓	8.92	↓	8.15	↓
	FMN	ESI^-	2.50	↓	5.97	↓	5.66	↓
	LPC (7:0)	ESI^+	2.14	↑				
	LPE (14:0)	ESI^+	1.47	↑	1.98	↑	2.07	↑
	LPE (16:0)	ESI^+			1.48	↑	1.51	↑
	LPG (16:0)	ESI^+	2.35	↑	4.65	↑	5.74	↑
O45	CMP-NeuGc	ESI^-	9.85	↓	317.61	↓	∞	↓
	CMP-NeuGc	ESI^-	6.67	↓	219.10	↓	∞	↓
	NAD^+	ESI^-	1.99	↓	140.37	↓	9324.74	↓
	ADP	ESI^+	7.40	↓	141.39	↓	∞	↓
	cADP-ribose	ESI^+	5.66	↓	71.19	↓	∞	↓
	cADP-ribose	ESI^-	2.93	↓	20.05	↓	198.37	↓
	NAD	ESI^+	6.96	↓	127.64	↓	2176.02	↓
	Adenine	ESI^+			12.03	↓	22.87	↓
	Dephospho-CoA	ESI^+	3.80	↓	322.61	↓	∞	↓
O103	CMP-Neu5Ac	ESI^-	9.83	↓	17.20	↓	43.94	↓
	CMP-Neu5Ac	ESI^-	6.48	↓	49.64	↓	22.26	↓
	CMP-NeuGc	ESI^-	6.65	↓	20.81	↓	38.19	↓
	CMP-NeuGc	ESI^-	4.56	↓	29.47	↓	69.72	↓
	NAD^+	ESI^-	2.03	↓	29.37	↓	104.64	↓
	cADP-ribose	ESI^+			8.01	↓	15.44	↓
	cADP-ribose	ESI^-	1.96	↓	5.51	↓	12.34	↓
	NAD	ESI^+	3.06	↓	17.56	↓	38.61	↓
	AMP	ESI^+	1.73	↑	3.36	↓	7.30	↓
	Pyridoxine	ESI^+	132.89	↓	97.46	↓	125.23	↓

(*continued on next page*)

Table 3 (*continued*)

Serotype	Metabolite	Polarity	AA		CA		MA	
			FC	Trend	FC	Trend	FC	Trend
	Dephospho-CoA	ESI^+			7.38	↓	22.09	↓
	Pantothenic acid	ESI^+	19.09	↓	33.59	↓	39.70	↓
	LPE (14:0)	ESI^+	3.32	↑	3.08	↑	3.14	↑
	LPE (16:1)	ESI^+	2.46	↑	2.59	↑	2.54	↑
	UDP-3-ketoglucose	ESI^-	1.76	↑	1.94	↑	1.98	↑
	LPE (16:0)	ESI^+	2.72	↑	2.67	↑	2.63	↑
	LPE (18:1)	ESI^+	2.53	↑	2.64	↑	2.59	↑
	LPG (16:0)	ESI^+	2.28	↑	2.20	↑		
O111	CMP	ESI^+					5.3	↓
	CMP-Neu5Ac	ESI^-	8.14	↓	9.34	↓	19.44	↓
	CMP-Neu5Ac	ESI^-	10.18	↓	47.25	↓	25.43	↓
	CMP-NeuGc	ESI^-	9.39	↓	22.67	↓	57.83	↓
	CMP-NeuGc	ESI^-	6.61	↓	30.26	↓	60.84	↓
	ADP	ESI^+	5.64	↓	15.60	↓	36.73	↓
	cADP-ribose	ESI^+	4.62	↓	11.90	↓	19.20	↓
	cADP-ribose	ESI^-	3.24	↓	5.19	↓	7.20	↓
	NAD	ESI^+	4.99	↓	12.96	↓	28.68	↓
	AMP	ESI^+			1.57	↓	5.72	↓
	Adenine	ESI^+			9.79	↓	27.29	↓
	Glutathione disulphide	ESI^+	24.96	↓	150.32	↓	∞	↓
	Adenosine	ESI^+	11.27	↓	48.97	↓	29.47	↓
	Dephospho-CoA	ESI^+					6.40	↓
	Coenzyme A	ESI^+	11.63	↓	∞	↓	∞	↓
	Pantothenic acid	ESI^+	26.98	↓	40.78	↓	163.94	↓
	LPE (14:0)	ESI^+	2.93	↑	8.30	↑	2.30	↑
	LPE (16:1)	ESI^+	2.78	↑	8.60	↓	9.86	↓
	LPE (18:1)	ESI^+	2.27	↑	2.35	↑	2.83	↓
	LPE (19:1)	ESI^+	2.30	↑	2.26	↑	1.91	↑
O121	CMP-Neu5Ac	ESI^-	9.37	↓	43.54	↓	7.81	↓
	CMP-NeuGc	ESI^-	4.35	↓	4.54	↓	6.11	↓
	CMP-NeuGc	ESI^-	2.89	↓	5.14	↓	4.48	↓
	ADP	ESI^+			26.30	↓		
	cADP-ribose	ESI^+	5.47	↓	19.18	↓	7.34	↓
	cADP-ribose	ESI^-	3.53	↓	5.48	↓	3.63	↓
	NAD	ESI^+	5.68	↓	29.75	↓	9.19	↓
	XDP	ESI^-			71.46	↑		
	AMP	ESI^+			6.46	↓	4.13	↓
	Adenine	ESI^+			13.23	↓		
	LPE (14:0)	ESI^+	1.91	↑	1.36	↓		
	LPE (19:1)	ESI^+	1.54	↑	1.55	↓		
O145	CMP-Neu5Ac	ESI^-	25.97	↓	34.49	↓	58.89	↓
	CMP-Neu5Ac	ESI^-	12.50	↓	112.39	↓	22.96	↓
	CMP-NeuGc	ESI^-	11.51	↓	39.14	↓	73.83	↓
	CMP-NeuGc	ESI^-	7.81	↓	40.51	↓	55.97	↓
	ADP	ESI^+	8.10	↓	28.79	↓	21.88	↓
	cADP-ribose	ESI^+	5.87	↓	21.08	↓	11.60	↓
	cADP-ribose	ESI^-	3.58	↓	7.49	↓	5.34	↓
	NAD	ESI^+	6.46	↓	24.95	↓	9.55	↓
	AMP	ESI^+	1.13	↑	3.18	↓	3.86	↓
	Coenzyme A	ESI^+	23.11	↓	∞	↓	∞	↓
	Pantothenic acid	ESI^+	28.37	↓	16.51	↓	4457.68	↓
	LPE (14:0)	ESI^+	1.66	↑				
	LPE (19:1)	ESI^+	1.64	↑	1.09	↑	1.30	↑

[a] AA: ascorbic acid; CA: citric acid; MA: malic acid; FC: fold change.

illustrating a decreased need for fatty acid synthesis and oxidation as well as energy production during the OA treatments (Leonardi et al., 2005). Apart from NAD, $NADP^+$ and FMN are also pivotally important enzyme cofactors in *E. coli*, which are most notable for their role in amino acid catabolism, beta-oxidation of fatty acids and electron transport (Foster & Moat, 1980; Mansoorabadi, Thibodeaux, & Liu, 2007). The reduced levels of these two compounds were observed in O26 specifically, revealing ulteriorly suppressed metabolic activities in the strain compared to the others. Such change led to more efficient energy allocation within the O26 cells, which might explain for the highest resistance of O26 amongst the strains towards the OA stresses.

In association with the impeded metabolic processes, a decreasing trend in adenine, adenine derivatives (adenosine, AMP, dAMP, ADP, and cADP-ribose), cytosine derivatives (CMP, CMP-Neu5Ac and CMP-NeuGc) as well as guanine derivatives (GMP, c-di-GMP and GDP-colitose) was observed in all *E. coli* strains, with the most extensive depletion still found in O26 (Fig. 5; Fig. 6). As these nucleotides are synthesised during DNA replication, cell division and cell growth, their reduced biosynthesis again, proposed retarded cell proliferation during the OA-stressed period (Bhat et al., 2015). Along with this pattern, higher levels of xanthine and hypoxanthine were generated from purine degradation as per the decreased nucleotide needs in cell multiplication. Besides, unlike the other nucleotides, uracil, together with its derivatives, showed an upward tendency after the OA treatments. Since uracil is only present in RNA, its change suggested a promoted RNA synthesis, potentially to be used for synthesising proteins and enzymes needed to function at low pH for acid resistance.

3.5.3. Amino acid metabolism

Amino acid decarboxylases and inner membrane antiporters, with

Metabolite	Detection means	O26			O45			O103			O111			O121			O145		
		AA	CA	MA	AA	CA	MA	AA	CA	MA	AA	CA	MA	AA	CA	MA	AA	CA	MA
Lipid metabolism																			
LPC(7:0)	ESI^+	↑																	
LPG(16:0)	ESI^+	↑	↑	↑				↑	↑										
LPE(14:0)	ESI^+	↑	↑	↑				↑	↑	↑	↑	↑	↑	↑	↓		↑		
LPE(16:0)	ESI^+		↑	↑				↑	↑	↑									
LPE(16:1)	ESI^+							↑	↑	↑	↑	↓	↓						
LPE(18:1)	ESI^+							↑	↑	↑	↑	↑	↓						
LPE(19:1)	ESI^+										↑	↑	↑	↑	↓		↑	↑	↑
Phosphorylcholine	NMR													↓			↓		
Amino acid metabolism																			
His	NMR		↓	↓	↓	↓	↓	↓	↓	↓	↓		↓	↓	↓	↓	↑		↓
Glu	NMR	↑		↑				↑		↑	↑	↑					↓	↓	↓
Arg	NMR							↑			↑			↑					↓
Leu	NMR	↑	↑	↑	↑	↑				↑	↑	↑		↓	↑	↑	↑	↑	↑
Ile	NMR	↑	↑	↑	↓	↓			↓				↓	↓	↓	↓	↑	↑	↓
Met	NMR	↑		↑		↓	↓	↑	↓	↓		↓	↓	↑		↓			↓
Phe	NMR					↑		↑											
Pyridoxine	ESI^+							↓	↓	↓									
Nucleotide metabolism																			
NAD	ESI^+	↓	↓	↓	↓	↓	↓	↓	↓	↓	↓	↓	↓	↓	↓	↓	↓	↓	↓
NAD^+	ESI^-				↓	↓	↓	↓	↓	↓									
$NADP^+$	ESI^+, ESI^-	↓	↓	↓															
FMN	ESI^+, ESI^-	↓	↓	↓															
Adenine	ESI^+	↓	↓	↓		↓	↓					↓	↓		↓				
Adenosine	NMR, ESI^+								↓		↓	↓	↓	↓					
AMP	ESI^+	↓	↓	↓				↑	↓	↓		↓	↓		↓	↓	↑	↓	↓
dAMP	ESI^+		↓	↓															
ADP	ESI^+	↓	↓	↓	↓	↓	↓				↓	↓	↓		↓		↓	↓	↓
cADP-ribose	ESI^+, ESI^-	↓	↓	↓	↓	↓	↓	↓	↓	↓	↓	↓	↓	↓	↓	↓	↓	↓	↓
CMP	ESI^+, ESI^-	↓	↓	↓									↓						
CMP-Neu5Ac	ESI^-	↓	↓	↓				↓	↓	↓	↓	↓	↓	↓	↓	↓	↓	↓	↓
CMP-NeuGc	ESI^-				↓	↓	↓	↓	↓	↓	↓	↓	↓	↓	↓	↓	↓	↓	↓
GMP	ESI^+		↓	↓															
c-di-GMP	ESI^-	↓	↓	↓															
GDP-colitose	ESI^-		↓	↓															
Xanthine	NMR	↑	↑	↑	↑	↑	↑	↑	↑	↑	↑	↑	↑	↑	↑	↑	↑	↑	↑
Hypoxanthine	NMR	↑	↑	↑	↑	↑	↑	↑	↑	↑	↑	↑	↑	↑	↑	↑	↑	↑	↑
XDP	ESI^-														↑				
Uracil	NMR	↑	↑	↑	↓					↑						↑		↑	↑
Uridine	NMR	↑	↑	↑	↑	↑	↑		↑	↑	↑	↑	↑	↑		↑		↑	↑
UDP-3-ketoglucose	ESI^-							↑	↑	↑									
Glucose metabolism																			
α-D-glucose	NMR				↓			↓			↓			↓					
Ethanol	NMR		↓	↓	↓	↑		↓	↓	↓	↑	↑	↑	↓	↑	↓		↑	
1,2-propanediol	NMR				↓									↓			↓		↓
Lactic acid	NMR	↑	↑	↑	↓	↓	↓	↑	↓	↑	↑	↑	↓	↓	↓	↓	↑	↑	↓
Acetic acid	NMR		↓	↓	↓	↓	↓	↓	↓	↓	↓	↓	↓	↓	↓	↓	↓	↓	↓
Coenzyme A synthesis																			
Pantothenic acid	ESI^+	↓	↓	↓				↓	↓	↓	↓	↓	↓				↓	↓	↓
Dephospho-CoA	ESI^+				↓	↓	↓		↓	↓			↓						
Coenzyme A	ESI^+, ESI^-	↓	↓	↓							↓	↓	↓		↓		↓	↓	↓
Others																			
Putrescine	NMR			↑	↑	↑	↑					↑	↓	↓	↓		↓	↑	↑
Glutathione disulphide	ESI^+	↓	↓	↓							↓	↓	↓						

Fig. 5. Significantly differential metabolites ($P < 0.05$) in *Escherichia coli* strains on pea sprouts from each organic acid treatment in comparison to the control detected by NMR and UPLC-MS.

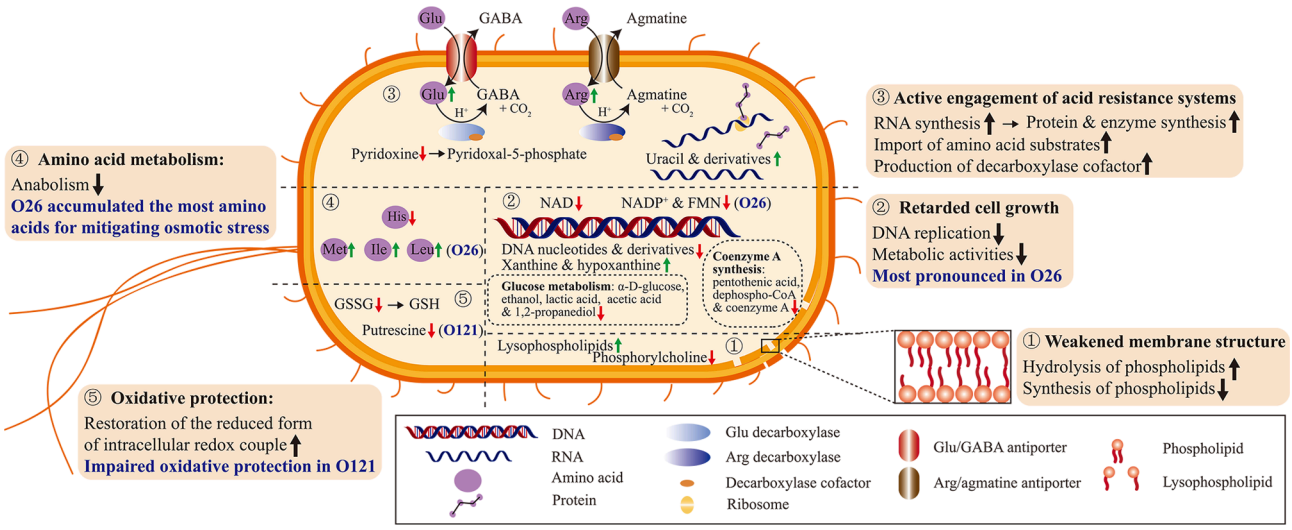

Fig. 6. Proposed schematic of metabolic alterations of organic acids against *Escherichia coli* strains on pea sprouts. Note: GSSG: glutathione disulphide; GSH: glutathione.

low pH optima, are amongst the most demanded enzymes and proteins under acidic conditions (Kanjee & Houry, 2013; Lund, Tramonti, & De Biase, 2014; Zhao et al., 2022). In *E. coli*, they constitute the amino acid-dependent acid resistance systems, where the cytoplasmic decarboxylases catalysing proton-dependent decarboxylation of substrate amino acids and the inner membrane substrate/product antiporters continuously exchanging internal product for external substrate work cooperatively for maintaining pH homeostasis (Foster, 2004; Kanjee & Houry, 2013). Glutamic acid-dependent acid resistance system and arginine-dependent acid resistance system are two of the acid resistance systems, which use glutamic acid and arginine as the substrate, respectively. In this study, an elevation in glutamic acid and/or arginine levels was observed in most of the strains (O26, O103, O111 and O121) (Fig. 5; Fig. 6), which indicated that the acid resistance processes were actively engaged in the *E. coli* strains to cope with OAs. Moreover, pyridoxal-5-phosphate is the cofactor of the decarboxylases (Kanjee & Houry, 2013); from the reduced level of pyridoxine in O103, the conversion of pyridoxine to pyridoxal-5-phosphate was likely promoted, which provided further evidence that the amino acid-dependent acid resistance systems were strongly induced by the OA treatments. Additionally, according to previous transcriptomic-based studies, the genes encoding decarboxylases and antiporters involved in the acid resistance systems are under the control of the stationary-phase sigma factor, RpoS (Castanie-Cornet et al., 1999; Lin et al., 1995). Therefore, echoing the down-regulation pattern of DNA nucleotides as mentioned in *3.5.2*, the stimulation of the acid resistance systems substantiated the *E. coli* strains' entry into the stationary phase.

Although less involved in the decarboxylation processes, other amino acids were also modulated during the stressed period. For example, a uniform decrease in histidine content was observed in all strains (Fig. 5; Fig. 6). This could be the result of an imbalanced amino acid anabolism and catabolism under the OA treatments, since the amino acid anabolic process is highly sensitive to hostile environmental conditions, such as heat, oxidation and acid (Jozefczuk et al., 2010; Wang, Wu, & Yang, 2022). Other discriminative amino acids included leucine, isoleucine and methionine, and they were all significantly accumulated in O26. Due to the fact that amino acids are natural osmolytes in *E. coli* (Wu et al., 2021), the massive amino acid accumulation might have helped with osmotic stress mitigation in the O26 cells, which contributed to the high OA-resistance of the O26 strain.

3.5.4. Oxidation protection

Metabolic changes relevant to oxidation protection were observed in the *E. coli* strains (Fig. 5; Fig. 6). According to previous studies, both low pH and hyper-osmolarity could co-induce oxidative damage to bacterial cells, due to the overlaps in bacterial genes stimulated by the three stresses (Maurer et al., 2005; Smirnova, Muzyka, & Oktyabrsky, 2000). Putrescine, through regulating the key adaptive response regulators (e.g., SoxR, SoxS and OxyR) to restore the reduced form of intracellular redox couples, plays an essential role in re-equilibrating the redox balance disturbed by the oxidative stress (Murray, Messner, & Kowdley, 2006; Tkachenko, Nesterova, & Pshenichnov, 2001). In this study, from the unchanged or decreased levels of glutathione disulphide observed in all six strains, it can be interpreted that putrescine was requisitioned in the oxidative stress defence mechanisms to convert glutathione disulphide back to glutathione. During this process, while putrescine was mostly retained in the other strains, it was significantly expended in O121 ($P < 0.05$). Exhaustion of putrescine undoubtedly impaired the oxidative protection in the strain, which potentially resulted in O121′s low resistance to OAs as was shown in *3.1*.

Overall, under the OA treatments, the metabolic perturbations in the "big six" strains were largely identical, whereas the minor differences in the strains' metabolic responses, such as variations in the levels of co-enzymes, amino acids and oxidative stress alleviator, contributed to the differential OA-resistance of the strains.

4. Conclusions

The effectiveness of OAs, especially MA, in mitigating "big six" *E. coli* strains on pea sprouts was manifested in this work. Through a dual-platform metabolomics investigation, metabolic changes implying a weakened cell membrane, activated amino acid decarboxylation and depressed cell activity were found to underlie the key antimicrobial mechanisms of the OA treatments. In addition, strain-specific metabolic changes, including ulteriorly suppressed cellular activity and large total amino acid accumulation, potentially contributed to O26's outstanding resistance to the OA stresses. Meanwhile, depletion of the oxidative stress regulator, putrescine, might explain for the lowest OA-resistance of the O121 strain. Overall, the study provides valuable insights into OAs' bactericidal activity against "big six" *E. coli* on pea sprouts, and the findings can serve as scientific basis for future OA application in fresh produce sanitisation.

CRediT authorship contribution statement

Yue Wang: Conceptualization, Data curation, Formal analysis,

Methodology, Investigation, Resources, Software, Visualization, Writing – original draft. **Xianfu Gao:** Formal analysis, Software, Writing – review & editing. **Hongshun Yang:** Conceptualization, Funding acquisition, Project administration, Supervision, Validation, Writing – review & editing.

Declaration of Competing Interest

The authors declare that they have no known competing financial interests or personal relationships that could have appeared to influence the work reported in this paper.

Acknowledgements

This study was funded by Applied Basic Research Project (Agricultural) Suzhou Science and Technology Planning Programme (SNG2020061), Singapore Ministry of Education Academic Research Fund Tier 1 (R-160-000-A40-114), and industry grants supported by Shanghai Cenwang Food Co., Ltd. (R-160-000-011-597) and Shanghai ProfLeader Biotech Co., Ltd (R-160-000-A21-597).

Appendix A. Supplementary material

Supplementary data to this article can be found online at https://doi.org/10.1016/j.foodres.2022.111354.

References

Alemohammad, M., & Knowles, C. J. M. (1974). Osmotically induced volume and turbidity changes of *Escherichia coli* due to salts, sucrose and glycerol, with particular reference to the rapid permeation of glycerol into the cell. *Microbiology, 82*(1), 125–142.

Allende, A., McEvoy, J., Tao, Y., & Luo, Y. (2009). Antimicrobial effect of acidified sodium chlorite, sodium chlorite, sodium hypochlorite, and citric acid on *Escherichia coli* O157:H7 and natural microflora of fresh-cut cilantro. *Food Control, 20*(3), 230–234.

Ashraf, S. A., Nazir, S., Adnan, M., & Azad, Z. R. A. A. (2020). UPLC-MS: An emerging novel technology and its application in food safety. In A. N. Srivastva (Ed.), *Analytical Chemistry - Advancement, Perspectives and Applications*. London: IntechOpen.

Beuchat, L. R., Mann, D. A., Kelly, C. A., & Ortega, Y. R. (2017). Retention of viability of *Salmonella* in sucrose as affected by type of inoculum, water activity, and storage temperature. *Journal of Food Protection, 80*(9), 1408–1414.

Bhat, S. V., Booth, S. C., Vantomme, E. A., Afroj, S., Yost, C. K., & Dahms, T. E. (2015). Oxidative stress and metabolic perturbations in *Escherichia coli* exposed to sublethal levels of 2,4-dichlorophenoxyacetic acid. *Chemosphere, 135*, 453–461.

Blessington, T., Theofel, C. G., & Harris, L. J. (2013). A dry-inoculation method for nut kernels. *Food Microbiology, 33*(2), 292–297.

Brul, S., & Coote, P. (1999). Preservative agents in foods. Mode of action and microbial resistance mechanisms. *International Journal of Food Microbiology, 50*(1–2), 1–17.

Burnett, S. L., & Beuchat, L. R. (2002). Comparison of methods for fluorescent detection of viable, dead, and total *Escherichia coli* O157:H7 cells in suspensions and on apples using confocal scanning laser microscopy following treatment with sanitizers. *International Journal of Food Microbiology, 74*(1), 37–45.

Castanie-Cornet, M. P., Penfound, T. A., Smith, D., Elliott, J. F., & Foster, J. W. (1999). Control of acid resistance in *Escherichia coli. Journal of Bacteriology, 181*(11), 3525–3535.

Centers for Disease Control and Prevention. (2012). O26 infections linked to raw clover sprouts at Jimmy John's Restaurants. https://www.cdc.gov/ecoli/2012/O26-02-12/index.html.

Centers for Disease Control and Prevention. (2014). O121 infections linked to raw clover sprouts. https://www.cdc.gov/ecoli/2014/o121-05-14/index.html.

Centers for Disease Control and Prevention. (2020). Outbreak of *E. coli* infections linked to clover sprouts. https://www.cdc.gov/ecoli/2020/o103h2-02-20/index.html.

Chen, L., Liu, Q., Zhao, X., Zhang, H., Pang, X., & Yang, H. (2022). Inactivation efficacies of lactic acid and mild heat treatments against *Escherichia coli* strains in organic broccoli sprouts. *Food Control, 133*, Article 108577.

Chen, L., Zhang, H., Liu, Q., Pang, X., Zhao, X., & Yang, H. (2019). Sanitising efficacy of lactic acid combined with low-concentration sodium hypochlorite on *Listeria innocua* in organic broccoli sprouts. *International Journal of Food Microbiology, 295*, 41–48.

Chen, L., Zhao, X., Wu, J., He, Y., & Yang, H. (2020a). Metabolic analysis of salicylic acid-induced chilling tolerance of banana using NMR. *Food Research International, 128*.

Chen, L., Zhao, X., Wu, J., Liu, Q., Pang, X., & Yang, H. (2020b). Metabolic characterisation of eight *Escherichia coli* strains including "Big Six" and acidic responses of selected strains revealed by NMR spectroscopy. *Food Microbiology, 88*, Article 103399.

Chung, D., Cho, T. J., & Rhee, M. S. (2018). Citrus fruit extracts with carvacrol and thymol eliminated 7-log acid-adapted *Escherichia coli* O157:H7, *Salmonella typhimurium*, and *Listeria monocytogenes*: A potential of effective natural antibacterial agents. *Food Research International, 107*, 578–588.

Cronan, J. E., Jr, & Wulff, D. L. J. V. (1969). A role for phospholipid hydrolysis in the lysis of *Escherichia coli* infected with bacteriophage T4. *Virology, 38*(2), 241–246.

de Geus, P., van Die, I., Bergmans, H., Tommassen, J., de Haas, G. J. M., & Mgg, g. g.. (1983). Molecular cloning of *pldA*, the structural gene for outer membrane phospholipase of *E. coli* K12. *Molecular and General Genetics MGG, 190*(1), 150–155.

Deng, K., Wang, S., Rui, X., Zhang, W., & Tortorello, M. L. (2011). Functional analysis of *ycfR* and *ycfQ* in *Escherichia coli* O157:H7 linked to outbreaks of illness associated with fresh produce. *Applied and Environmental Microbiology, 77*(12), 3952–3959.

Dewey-Mattia, D., Kisselburgh, H., Manikonda, K., Silver, R., Subramhanya, S., Sundararaman, P., Whitham, H., & Crowe, S. (2019). Surveillance for foodborne disease outbreaks, United States, 2017 annual report. In. Atlanta, Georgia, U.S.: Centers for Disease Control and Prevention.

Dewey-Mattia, D., Manikonda, K., Hall, A. J., Wise, M. E., & Crowe, S. J. (2018). Surveillance for foodborne disease outbreaks - United States, 2009-2015. *Morbidity and Mortality Weekly Report. Surveillance Summaries, 67* (10), 1-11.

Dong, W. R., Sun, C. C., Zhu, G., Hu, S. H., Xiang, L. X., & Shao, J. Z. (2014). New function for *Escherichia coli* xanthosine phophorylase (*xapA*): Genetic and biochemical evidences on its participation in NAD^+ salvage from nicotinamide. *BMC Microbiology, 14*(1), 29.

Emwas, A. H. (2015). The strengths and weaknesses of NMR spectroscopy and mass spectrometry with particular focus on metabolomics research. In B. J. (Ed.), *Metabonomics. Methods in Molecular Biology*. (2015/02/14 ed., Vol. 1277, pp. 161-193): Humana Press, New York, NY.

Fang, T. J., & Tsai, H.-C. (2003). Growth patterns of *Escherichia coli* O157:H7 in ground beef treated with nisin, chelators, organic acids and their combinations immobilized in calcium alginate gels. *Food Microbiology, 20*(2), 243–253.

Food and Drug Administration. (2022). Investigations of foodborne illness outbreaks. https://www.fda.gov/food/outbreaks-foodborne-illness/investigations-foodborne-illness-outbreaks.

Foster, J. W. (2004). *Escherichia coli* acid resistance: Tales of an amateur acidophile. *Nature Reviews: Microbiology, 2*(11), 898–907.

Foster, J. W., & Moat, A. G. (1980). Nicotinamide adenine dinucleotide biosynthesis and pyridine nucleotide cycle metabolism in microbial systems. *Microbiological reviews, 44*(1), 83–105.

Geiger, O., López-Lara, I. M., & Sohlenkamp, C. (2013). Phosphatidylcholine biosynthesis and function in bacteria. *Biochimica et Biophysica Acta (BBA) - Molecular and Cell Biology of Lipids, 1831*(3), 503–513.

Gray, D. A., Dugar, G., Gamba, P., Strahl, H., Jonker, M. J., & Hamoen, L. W. (2019). Extreme slow growth as alternative strategy to survive deep starvation in bacteria. *Nature Communications, 10*(1), 890.

Guo, C., He, Y., Wang, Y., & Yang, H. (2022). NMR-based metabolomic investigation on antimicrobial mechanism of *Salmonella* on cucumber slices treated with organic acids. *Food Control, 137*, Article 108973.

Haskard, C., Binnion, C., & Ahokas, J. (2000). Factors affecting the sequestration of aflatoxin by *Lactobacillus rhamnosus* strain GG. *Chemico-Biological Interactions, 128* (1), 39–49.

He, Y., Zhao, X., Chen, L., Zhao, L., & Yang, H. (2021). Effect of electrolysed water generated by sodium chloride combined with sodium bicarbonate solution against *Listeria innocua* in broth and on shrimp. *Food Control, 127*, Article 108134.

Jain, R., Sun, X., Yuan, Q., & Yan, Y. (2015). Systematically engineering *Escherichia coli* for enhanced production of 1,2-propanediol and 1-propanol. *ACS Synthetic Biology, 4* (6), 746–756.

Jäpelt, K. B., Nielsen, N. J., Wiese, S., & Christensen, J. H. (2015). Metabolic fingerprinting of *Lactobacillus paracasei*: A multi-criteria evaluation of methods for extraction of intracellular metabolites. *Analytical and Bioanalytical Chemistry, 407* (20), 6095–6104.

Ji, F., Shen, Y., Tang, L., & Cai, Z. (2018). Determination of intracellular metabolites concentrations in *Escherichia coli* under nutrition stress using liquid chromatography-tandem mass spectrometry. *Talanta, 189*, 1–7.

Jozefczuk, S., Klie, S., Catchpole, G., Szymanski, J., Cuadros-Inostroza, A., Steinhauser, D., … Willmitzer, L. (2010). Metabolomic and transcriptomic stress response of *Escherichia coli*. *Molecular Systems Biology, 6*(1), 364.

Kanjee, U., & Houry, W. A. (2013). Mechanisms of acid resistance in *Escherichia coli*. *Annual Review of Microbiology, 67*, 65–81.

Kempes, C. P., van Bodegom, P. M., Wolpert, D., Libby, E., Amend, J., & Hoehler, T. (2017). Drivers of bacterial maintenance and minimal energy requirements. *Frontiers in Microbiology, 8*.

Kharel, K., Adhikari, A., Graham, C. J., Prinyawiwatkul, W., & Yemmireddy, V. K. (2018). Hot water treatment as a kill-step to inactivate *Escherichia coli* O157:H7, *Salmonella enterica*, *Listeria monocytogenes* and *Enterococcus faecium* on in-shell pecans. *LWT - Food Science and Technology, 97*, 555–560.

Leonardi, R., Zhang, Y.-M., Rock, C. O., & Jackowski, S. (2005). Coenzyme A: Back in action. *Progress in Lipid Research, 44*(2), 125–153.

Lin, J., Lee, I. S., Frey, J., Slonczewski, J. L., & Foster, J. W. (1995). Comparative analysis of extreme acid survival in *Salmonella typhimurium*, *Shigella flexneri*, and *Escherichia coli*. *Journal of Bacteriology, 177*(14), 4097–4104.

Lin, L., Dai, S., Tian, B., Li, T., Yu, J., Liu, C., … Hua, Y. (2016). DqsIR quorum sensing-mediated gene regulation of the extremophilic bacterium *Deinococcus radiodurans* in response to oxidative stress. *Molecular Microbiology, 100*(3), 527–541.

Lioupi, A., Marinaki, M., Virgiliou, C., Gika, H., Wilson, I., & Theodoridis, G. (2021). Chapter 1 State-of-the-art in LC–MS approaches for probing the polar metabolome.

In *Advanced Mass Spectrometry-based Analytical Separation Techniques for Probing the Polar Metabolome* (pp. 1–26). The Royal Society of Chemistry.
Liu, Q., Chen, L., Lasernab, A., He, Y., Feng, X., & Yang, H. (2020). Synergistic action of electrolyzed water and mild heat for enhanced microbial inactivation of *Escherichia coli* O157:H7 revealed by metabolomics analysis. *Food Control, 110*, Article 107026.
Liu, Q., Wu, J., Lim, Z. Y., Aggarwal, A., Yang, H., & Wang, S. (2017). Evaluation of the metabolic response of *Escherichia coli* to electrolysed water by 1H NMR spectroscopy. *LWT - Food Science and Technology, 79*, 428–436.
Loh, L. X., Ng, D. H. J., Toh, M., Lu, Y., & Liu, S. Q. (2021). Targeted and nontargeted metabolomics of amino acids and bioactive metabolites in probiotic-fermented unhopped beers using liquid chromatography high-resolution mass spectrometry. *Journal of Agricultural and Food Chemistry, 69*(46), 14024–14036.
Lou, X., Zhai, D., & Yang, H. (2020). Changes of metabolite profiles of fish models inoculated with *Shewanella baltica* during spoilage. *Food Control, 123*(2), Article 107697.
Lund, P., Tramonti, A., & De Biase, D. (2014). Coping with low pH: Molecular strategies in neutralophilic bacteria. *FEMS Microbiology Reviews, 38*(6), 1091–1125.
Mansoorabadi, S. O., Thibodeaux, C. J., & Liu, H. (2007). The diverse roles of flavin coenzymes–nature's most versatile thespians. *The Journal of organic chemistry, 72*(17), 6329–6342.
Maurer, L. M., Yohannes, E., Bondurant, S. S., Radmacher, M., & Slonczewski, J. L. (2005). pH regulates genes for flagellar motility, catabolism, and oxidative stress in *Escherichia coli* K-12. *Journal of Bacteriology, 187*(1), 304–319.
Mille, Y., Beney, L., & Gervais, P. (2002). Viability of *Escherichia coli* after combined osmotic and thermal treatment: a plasma membrane implication. *Biochimica et Biophysica Acta (BBA) - Biomembranes, 1567*, 41-48.
Min, J. S., Lee, S. O., Jang, A., Jo, C., & Lee, M. (2007). Control of microorganisms and reduction of biogenic amines in chicken breast and thigh by irradiation and organic acids. *Poultry Science, 86*(9), 2034–2041.
Murray, K. F., Messner, D. J., & Kowdley, K. V. (2006). Chapter 58 - Mechanisms of hepatocyte detoxification. In L. R. Johnson (Ed.), *Physiology of the Gastrointestinal Tract* (Fourth Edition, pp. 1483–1504). Burlington: Academic Press.
Neal, J. A., Marquez-Gonzalez, M., Cabrera-Diaz, E., Lucia, L. M., O'Bryan, C. A., Crandall, P. G., … Castillo, A. (2012). Comparison of multiple chemical sanitizers for reducing *Salmonella* and *Escherichia coli* O157:H7 on spinach (*Spinacia oleracea*) leaves. *Food Research International, 45*(2), 1123–1128.
Olaimat, A. N., Al-Holy, M. A., Abu Ghoush, M. H., Al-Nabulsi, A. A., Osaili, T. M., Ayyash, M., … Holley, R. A. (2022). Use of citric acid and garlic extract to inhibit *Salmonella enterica* and *Listeria monocytogenes* in hummus. *International Journal of Food Microbiology, 362*, Article 109474.
Olaimat, A. N., Al-Nabulsi, A. A., Osaili, T. M., Al-Holy, M., Ayyash, M. M., Mehyar, G. F., … Ghoush, M. A. (2017). Survival and inhibition of *Staphylococcus aureus* in commercial and hydrated tahini using acetic and citric acids. *Food Control, 77*, 179–186.
Ozment, C., Barchue, J., DeLucas, L. J., & Chattopadhyay, D. (1999). Structural study of *Escherichia coli* NAD synthetase: Overexpression, purification, crystallization, and preliminary crystallographic analysis. *Journal of Structural Biology, 127*(3), 279–282.
Park, S. H., Choi, M. R., Park, J. W., Park, K. H., Chung, M. S., Ryu, S., & Kang, D. H. (2011). Use of organic acids to inactivate *Escherichia coli* O157:H7, *Salmonella* Typhimurium, and *Listeria monocytogenes* on organic fresh apples and lettuce. *Journal of Food Science, 76*(6), M293–M298.
Rekhy, R., & McConchie, R. (2014). Promoting consumption of fruit and vegetables for better health. Have campaigns delivered on the goals? *Appetite, 79*, 113–123.
Russell, J. B. (1992). Another explanation for the toxicity of fermentation acids at low pH: anion accumulation versus uncoupling. *73* (5), 363-370.
Salmond, C. V., Kroll, R. G., & Booth, I. R. (1984). The effect of food preservatives on pH homeostasis in *Escherichia coli*. *Journal of General Microbiology, 130*(11), 2845–2850.
Sellick, C. A., Hansen, R., Stephens, G. M., Goodacre, R., & Dickson, A. J. (2011). Metabolite extraction from suspension-cultured mammalian cells for global metabolite profiling. *Nature Protocols, 6*(8), 1241–1249.
Shen, C., Geornaras, I., Belk, K. E., Smith, G. C., & Sofos, J. N. (2011). Thermal Inactivation of acid, cold, heat, starvation, and desiccation stress–adapted *Escherichia coli* O157:H7 in moisture-enhanced nonintact Beef. *Journal of Food Protection, 74*(4), 531–538.
Smirnova, G. V., Muzyka, N. G., & Oktyabrsky, O. N. (2000). The role of antioxidant enzymes in response of *Escherichia coli* to osmotic upshift. *186* (2), 209-213.
Tepperman, B. L., & Soper, B. D. (1999). The role of phospholipase A2 in calcium-ionophore-mediated injury to rat gastric mucosal cells. *Digestive Diseases and Sciences, 44*(3), 494–502.
Tian, X., Yu, Q., Yao, D., Shao, L., Liang, Z., Jia, F., … Dai, R. (2018). New insights Into the response of metabolome of *Escherichia coli* O157:H7 to ohmic heating. *Frontiers in Microbiology, 9*(2936).
Tkachenko, A., Nesterova, L., & Pshenichnov, M. (2001). The role of the natural polyamine putrescine in defense against oxidative stress in *Escherichia coli*. *Archives of Microbiology, 176*(1–2), 155–157.
Wang, S., Deng, K., Zaremba, S., Deng, X., Lin, C., Wang, Q., … Zhang, W. (2009). Transcriptomic response of *Escherichia coli* O157:H7 to oxidative stress. *Applied and Environmental Microbiology, 75*(19), 6110–6123.
Wang, Y., Wu, J., & Yang, H. (2022). Comparison of the metabolic responses of eight *Escherichia coli* strains including the "big six" in pea sprouts to low concentration electrolysed water by NMR spectroscopy. *Food Control, 131*, Article 108458.
Wang, Y., Zhou, D., & Yang, H. (2022). Metabolic responses of "big six" *Escherichia coli* in wheat flour to thermal treatment revealed by nuclear magnetic resonance spectroscopy. *Applied and Environmental Microbiology, 88*(7), e00098–00022.
Weiss, J., Beckerdite-Quagliata, S., & Elsbach, P. (1979). Determinants of the action of phospholipases A on the envelope phospholipids of *Escherichia coli*. *Journal of Biological Chemistry, 254*(21), 11010–11014.
Wiklund, S., Johansson, E., Sjöström, L., Mellerowicz, E. J., Edlund, U., Shockcor, J. P., … Trygg, J. (2008). Visualization of GC/TOF-MS-Based metabolomics data for identification of biochemically interesting compounds using OPLS class models. *Analytical Chemistry, 80*(1), 115–122.
Winder, C. L., Dunn, W. B., Schuler, S., Broadhurst, D., Jarvis, R., Stephens, G. M., & Goodacre, R. (2008). Global metabolic profiling of *Escherichia coli* cultures: An evaluation of methods for quenching and extraction of intracellular metabolites. *Analytical Chemistry, 80*(8), 2939–2948.
Wood, J. M. (1999). Osmosensing by bacteria: Signals and membrane-based sensors. *Microbiology and Molecular Biology Reviews, 63*(1), 230–262.
World Health Organization. (2003). Diet, nutrition, and the prevention of chronic diseases: report of a joint WHO/FAO expert consultation (Vol. 916). In. Geneva, Switzerland.
World Health Organization. (2014). European food and nutrition action plan 2015–2020. In. Copenhagen, Denmark.
Wright, G. C., Weiss, J., Kim, K. S., Verheij, H., & Elsbach, P. (1990). Bacterial phospholipid hydrolysis enhances the destruction of *Escherichia coli* ingested by rabbit neutrophils. Role of cellular and extracellular phospholipases. *The Journal of Clinical Investigation, 85*(6), 1925–1935.
Wu, J., Zhao, L., Lai, S., & Yang, H. (2021). NMR-based metabolomic investigation of antimicrobial mechanism of electrolysed water combined with moderate heat treatment against *Listeria monocytogenes* on salmon. *Food Control, 125*, Article 107974.
Zhang, H., Dolan, H. L., Ding, Q., Wang, S., & Tikekar, R. V. (2019). Antimicrobial action of octanoic acid against *Escherichia coli* O157:H7 during washing of baby spinach and grape tomatoes. *Food Research International, 125*, Article 108523.
Zhao, L., Poh, C. N., Wu, J., Zhao, X., He, Y., & Yang, H. (2022). Effects of electrolysed water combined with ultrasound on inactivation kinetics and metabolite profiles of *Escherichia coli* biofilms on food contact surface. *Innovative Food Science & Emerging Technologies, 76*, Article 102917.
Zhao, X., Chen, L., Wu, J., He, Y., & Yang, H. (2020). Elucidating antimicrobial mechanism of nisin and grape seed extract against *Listeria monocytogenes* in broth and on shrimp through NMR-based metabolomics approach. *International Journal of Food Microbiology, 319*, Article 108494.
Zhao, X., Wu, J., Chen, L., & Yang, H. (2019). Effect of vacuum impregnated fish gelatin and grape seed extract on metabolite profiles of tilapia (*Oreochromis niloticus*) fillets during storage. *Food Chemistry, 293*, 418–428.
Zheng, L., Lin, Y., Lu, S., Zhang, J., & Bogdanov, M. (2017). Biogenesis, transport and remodeling of lysophospholipids in Gram-negative bacteria. *Biochimica et Biophysica Acta (BBA) - Molecular and Cell Biology of Lipids, 1862*(11), 1404–1413.